SkyTEM survey Antartica 2011 - HydroGeophysics Group - Aarhus University

SkyTEM survey Antartica 2011

Report number 06-07-2015, June 2015

HydroGeophysics Group
AARHUS UNIVERSITY

Table of Contents

1. PROJECT SUMMARY

The SkyTEM Antarctica project is part of the United States Antarctica Program, organized by the American agency National Science Foundation (NSF). The SkyTEM survey consists of several areas around McMurdo valleys, which is the largest relatively ice-free area (approximately 4,800 square kilometers) on the Antarctic continent (Figure 1). This is why the term “dry valleys” is used.

People involved in this project are distributed into two groups: McMurdo Dry Valleys Long-Term Ecological Research (MCM LTER) which studies climate change on ecosystems, a

nd Whillans Ice Stream Subglacial Access Research Drilling (WISSARD) which studies subglacial life habitats in Antarctica.

This project has several goals:

- Mapping the geology of this unique valley system, so that MCM LTER can give hypothesis about the story of its formation
- Finding geothermal connections between marine system and an active volcano (Ross Island area)
- Study of the microbial ecosystem and its relationships with surface structures in sub glacial environment (Taylor Glacier).

This last and main objective is focused on the Taylor Glacier, where Blood Falls release red brine thanks to a fault. Indeed, studying those isolated microbial ecosystems will help to understand previous microbial life forms on Earth as well as potential life on other planets having similar conditions. As ice is a very special biologic stressor, novel enzymes and metabolic strategies could also be found thanks to this study. This brine shows microbial activity and is supposed to flow below the glacier and above the bedrock. SkyTEM aims to describe it as accurately as possible.

Few months after the survey a master student, Guillaume-Alexandre Sab, worked on the processing of the data as part of his master thesis (Sab, 2012). Since no cultural or man-made noises exist in the area, the usual culling of the coupled data was not necessary. However, since the resistivities are locally very high (above thousands Ωm for ice or frozen permafrost), a careful analysis was necessary to separate what is signal and noise, and so to remove the noisy parts to avoid interpretation of fictive conductive targets.

The survey was flown in Nov.-Dec. 2011. Preliminary results were presented during a meeting in Denver (May 2012) and Guillaume finished the processing before ending his master thesis at the end of August 2012. First complete results of SCIs were sent to US partners at the end of November 2012.

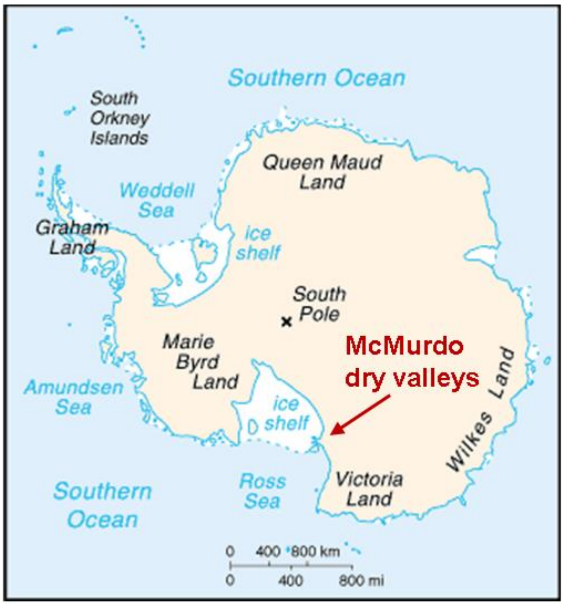

Figure 1. Antarctica map locating McMurdo dry valleys (source: www.cia.gov).

SkyTEM survey Antarctica 2011	
Client	American agency National Science Foundation (NSF)
Contact persons	Esben Auken, Aarhus University
Locality	McMurdo, Dry valleys, Antarctica
Field Period	November 28th to December 9th, 2011
Line km planned	1000 km
Line km acquired	1000 km
Line separation	~ 300 m
Average flight speed	~10 m/s
Average flight altitude (frame height)	30 m above the ground (higher in some places where slopes of the valleys are very steep)

Table 1. Project summary.

2. INTRODUCTION

As mentioned in part 1 of this report, the main difficulty encountered in the processing of the data was the signal-to-noise ratio which is very poor in some places where no conductor is present. Careful identification between noise, earth response, and also coil (or system) response (CR) has been necessary. Above the most very resistive places (e.g. frozen permafrost, or very thick part of glaciers) the only coherent signal observable was the CR. For such AEM soundings the data were simply removed before inversion. In some places, it can also happen that first gates are more noisy than intermediate ones as conductor (here mainly salt water) is deeply buried below a thick resistor, which implies a time delay in the EM response.

The main target observable across the different areas of the survey (see details in Chapter 4 about data collection) is saltwater, below glacier or as saltwater intrusion on the edge of the volcano at Ross Island, or even as hyper-saline water (more conductive than sea water) within and below the lakes of the dry valleys. In places where there is no presence of nearby conductors, it is almost possible to distinguish between the ice (clearly above 10.000 Ωm) and the frozen permafrost (>1.000 Ωm). Where the permafrost starts to unfreeze a resistivity gradient toward lower resistivity values can be observed. A conductivity water log in one of the lake (Lake Bonney) has shown a resistivity gradient (toward very low resistivity values with the sedimentation of the salt in the bottom) very similar to the one estimated with SkyTEM data. The bottom of the hyper-saline lakes is though impossible to distinguish from the sediments highly saturated with saltwater in AEM data, because of the similar high conductive values.

In this report no results are presented. The results and interpretations can be viewed in Mikucki et al, 2015. This report presents the results and documents the processing and the inversion of the data. Chapter 3 gives a quick overview of the different steps in the project. Chapters 4 - 6 describe the data collection, processing and inversion. Chapter 7 introduces the geophysical maps and cross-sections which has been used for MMikucki et al. 2014. Chapter 8 concludes the report. **Appendix I** contains Quality Control (QC) maps, and **Appendix II**: describes the Aarhus Workbench workspaces that hold the inversion results of both areas. Upon request, the Aarhus Workbench workspaces can be delivered.

Project management: Professor, Esben Auken, PhD.
Data processing and reporting:
M.Sc. Jesper Bjergsted Pedersen

Postdoc, Giulio Vignoli, PhD

Master student, Guillaume-Alexandre Sab

Postdoc, Cyril Schamper, PhD.

3. PROJECT TIMELINE

Table 2 shows a schematic view of the different steps in the project.

Collection of data
The field campaign was performed in from 28/11/2011 to 09/12/2011, and high-quality SkyTEM data were obtained.

Data processing
The collected data were then carefully processed to remove couplings and noise before the inversion.

Inversion
After processing and preliminary inversions the data have been inverted using the spatially constrained inversion (SCI) approach.

Processing steps and meeting
Few months after the survey a master student, Guillaume-Alexandre Sab, worked on the processing of the data as part of his master thesis (Sab, 2012). Since no cultural or man-made noises exist in the area, the usual culling of the coupled data was not necessary. However, since the resistivities are very high (above thousands Ωm) at all depth a careful analysis was necessary to separate what is signal and noise, and so to remove the noisy parts to avoid interpretation of fictive conductive targets.

Preliminary results were presented during a meeting in Denver (May 2012) and Guillaume finished the processing before ending his master thesis at the end of August 2012. First complete results of SCIs were sent to US partners at the end of November 2012.

2011	2012				2013
Nov.-Dec.	March-April	April	May-August	Nov.-Dec.	June-July
Survey	1st processing phase	Denver meeting	Final processing	Results of SCIs sent to US partners	Re-run of SCIs with improved parameters + new sending to US partners

Table 2 Antarctica project timeline

4. DATA COLLECTION

4.1 The survey area

The full survey (from 28/11/2011 to 09/12/2011) represents 1000 line km (621 miles) of resistivity profiles, covering an area of approximately 295 km² (114 square miles) displayed in Figure 2 where flight lines are visible. The survey can be divided into 4 main areas:

• Taylor Valley: The biggest area in term of flights and number of soundings. This is the area where signal quality is the best.

• Taylor Glacier: Ice rapidly lowers S/N ratio (it is the most resistive element we can find in the data), but it is the most important area. There is a lot of expectations concerning micro-biological research and modeling, one the main goal of the project.

• Ross Island: Volcanic formations rapidly lower S/N ratio as well, but the goal is to see if there is connection between volcano and marine systems.

• Dry valleys (including Lake Vida and Lake Vanda): This area concerns Wright Valley, mainly permafrost formed so where S/N ratio is not good, and two lakes: Lake Vanda South-West and Lake Vanda North-East, where S/N ratio is very good because of the hyper salinity of the lakes.

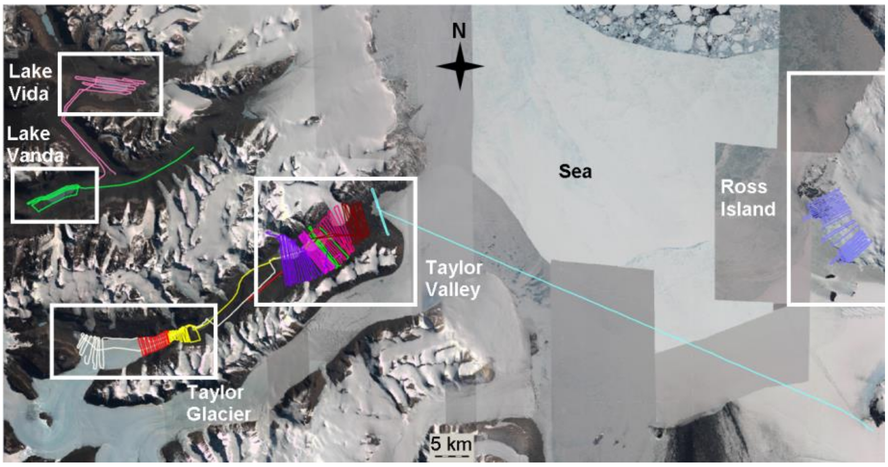

Figure 2. The different areas flown during the survey

4.2 Overview of the SkyTEM system

SkyTEM is a time-domain helicopter borne electromagnetic system designed for hydrogeophysical, environmental and mineral investigations. The following contains a general introduction to the SkyTEM system. A more thorough description of the SkyTEM method is found in (Sørensen and Auken, 2004). A description of the TEM method in general can be found in Jørgensen et al. (2003) and Nabighian and Macnae (1991).

For the present survey the largest and most powerful version of SkyTEM system was used, the SkyTEM 508 system (Figure 3), to ensure the deepest depth of penetration possible. This is particularly important for Taylor Glacier sub-area (cf. location in Figure 2) where a deep conductor has been successfully detected up to below 400 m of ice. More upstream in the glacier the ice was too thick to get a reliable signal. Future ground-based TEM survey is considered to investigate at so large depths.

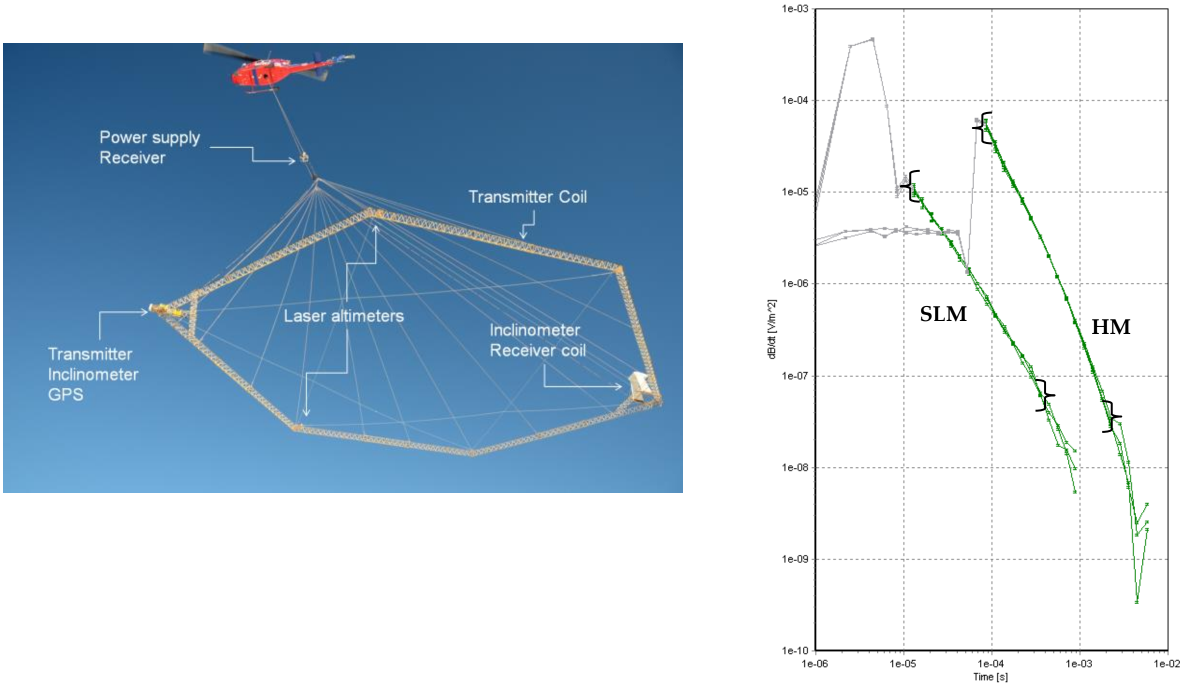

Figure 3. Left: The SkyTEM 508 system in operation. Right: a typical db/dt sounding curve from SkyTEM system with both Super Low (SLM) and High (HM) moment curves. This sounding example is before stack and located above one of the lake of the Dry Valleys. In places where no near-surface conductor is present, it generally results in no signal in SLM and a of a delayed TEM response in HM if a deep conductor is present. Braces indicate the gates that are commonly used in the different moments for the inversion. The gates actually used in each sub-area highly depend on the local resistivity values which can be very different from one area to another.

Instrument

Figure 3 shows a picture of the SkyTEM 508 system with the hexagonal frame below the helicopter. The lengths of the frame sides are approximately 16 m. The transmitter loop is mounted on the frame in an octagonal polygon configuration. The receiver loop is placed approximately 2 m above the frame in what is roughly a central loop configuration with a vertical offset. Two lasers placed on the frame measure the distance to terrain continuously while flying, and two inclinometers measure the tilt of the frame. Power is supplied by a generator placed between the helicopter and the frame. The positions of the different devices on the frame are shown in Figure 3 and Figure 4.

Measurement procedure

The configuration of the system is customized for each survey. Measurements are carried out with one or two transmitter moments, depending on the target geology. The standard configuration uses a low and a high transmitter moment applied sequentially. Each SLM sequence has 256 individual transient measurements, and each HM sequence corresponds to 64 measurements. Background noise is measured every 10 soundings (each one composed of both SLM and HM sequences).

The flight altitude is depending on flight speed, topography, etc. A typical nominal flight altitude is 30-50 m. When topography is varying a lot, the helicopter has to take larger and safer clearance from the ground. Also the altitude can be larger at the beginning and at the end of a flight line due to pilot maneuvers. The operating speed is customized to the survey area and target. The nominal speed for the SkyTEM 508 system was set to 36 km/h for the present survey.

Apart from GPS-, altitude- and TEM data, a number of instrument parameters are monitored and stored digitally in order to be used for quality control when the data are processed.

Penetration depth

The penetration depth for the SkyTEM system depends on the moment, the geological conditions, the level of the background noise and the speed and altitude of the frame. The influence of the latter is important, and in order to achieve good data, the altitude should normally be less than 50 m. A penetration depth down to approximately 400 m can be achieved for the present SkyTEM 508 system, especially where large thickness of ice (Taylor Glacier) of frozen permafrost is present in the top. During the inversion a depth of investigation is estimated for each resistivity model (see section 6.3).

4.3 SkyTEM – technical specifications

The SkyTEM 508 system was configured in a standard two-moment setup (super low moment, SLM and high moment, HM) to obtain a full dB/dt decay curve (sounding curve, cf. example in Figure 3). This version of SkyTEM system is the largest one in terms of transmitter size and moment. Such a big system is mandatory to be able to get a sufficiently good signal-to-noise ratio at late times for deep buried targets.

The system instrument setup is shown in

Figure 4. The positioning of the instruments and the corners of the octagon described by the transmitter coil are found in Table 3. The origin is defined as the center of the transmitter coil.

The parameters for the measured moments are summarized in Table 4. The receiver coil and the receiver instrument are modeled using first order low-pass filters with the values shown in Table 7.

Gate and receiver specifications are summarized in Table 8 and Table 9.

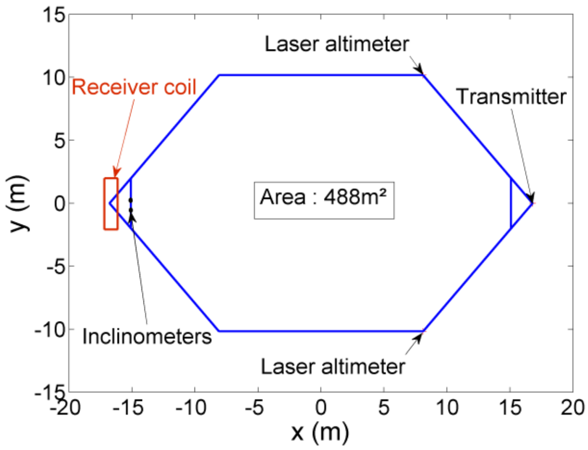

Figure 4. Instrument setup for the SkyTEM system used. Power supply and recording instruments were held right above the transmitter frame at mid-distance between the loop and the helicopter (cf. Figure 3).

Unit	X (m)	Y (m)	Z(m)
GPS1	16.5	1.00	-0.10
GPS2	14.0	2.00	-0.30
HE 1 (Altimeter)	4.75	7.31	0.00
HE 2 (Altimeter)	4.75	-7.31	0.00
TL 1 (inclinometer)	-15.0	-0.50	-0.16
TL 2 (inclinometer)	-15.0	0.15	-0.30
Rx (Receiver Coil)	-17.0	0.00	-1.90
Tx (Transmitter Coil)	0.00	0.00	0.00
Loop corner 1	-15.09	-2.00	0.00
Loop corner 2	-8.11	-10.16	0.00
Loop corner 3	8.11	-10.16	0.00
Loop corner 4	15.09	-2.00	0.00
Loop corner 5	15.09	2.00	0.00
Loop corner 6	8.11	10.16	0.00
Loop corner 7	-8.11	10.16	0.00
Loop corner 8	-15.09	2.00	0.00

Table 3. Summary of equipment and transmitter coil corner positioning. The origin is defined as the center of the transmitter coil. Z is negative towards the helicopter.

Parameter	SLM	HM
No. of turns	1	4
Area	488 m^2	488 m^2
Current	~ 9.45 A	~ 94.5 A
Tx Moment	~ 4 612 Am^2	~ 184 464 Am^2
Repetition frequency, Transients in full sign pattern	30 Hz , 16 repetitions of (+1 +1 +1 +1 +1 +1 +1 +1 - 1 -1 -1 -1 -1 -1 -1 -1)	30 Hz , 32 repetitions of (+1 -1)
Tx-on-time	1.00E-3 s	10.00E-3 s
Tx-off-time	7.16E-6 s	57.6E-6 s
Waveform	Square	Square
Turn-on exp. decay constant	See Table 5	See Table 6
Turn-off linear ramp	See Table 5	See Table 6
Turn-off current at end of avalanche mode	See Table 5	See Table 6
Turn-off free decay exp. constant	See Table 5	See Table 6

Table 4. Summary of SLM and HM specifications.

Time (s)	Normalized current
-1.00E-03	0.000E+00
-9.80E-04	4.645E-01
-9.55E-04	7.917E-01
-9.20E-04	9.369E-01
-9.10E-04	9.548E-01
-8.00E-04	1.000E+00
0.00E+00	1.000E+00
4.40E-07	9.841E-01
8.00E-07	9.344E-01
1.10E-06	8.688E-01
1.58E-06	6.899E-01
2.16E-06	4.582E-01
2.94E-06	2.159E-01
3.90E-06	7.150E-02
5.34E-06	1.300E-02
6.48E-06	3.900E-03
7.16E-06	0.000E+00

Table 5. Piece-linear description of the SLM waveform.

Time (s)	Normalized current
-1.00E-02	0.000E+00
-8.70E-03	3.604E-01
-7.10E-03	6.418E-01
-5.50E-03	8.505E-01
-3.30E-03	9.288E-01
-1.20E-03	9.825E-01
-5.00E-05	1.000E+00
0.00E+00	1.000E+00
3.70E-06	9.397E-01
1.57E-05	7.175E-01
3.08E-05	4.254E-01
4.22E-05	2.116E-01
5.09E-05	5.000E-03
5.50E-05	3.000E-03
5.76E-05	0.000E+00

Table 6. Piece-linear description of the HM waveform.

Filters	Frequency (kHz)
Receiver Coil	450
Receiver Instrument	300

Table 7. Low-pass filters for the entire survey.

Gate No.	Gate center time*	Gate start time*	Gate center time after calibration for SLM	Gate center time after calibration for HM	Gate width	SLM	HM
1	1.195E-06	3.900E-07	4.950e-007	-1.805e-006	1.610E-06		
2	3.195E-06	2.390E-06	2.495e-006	1.950e-007	1.610E-06		
3	5.195E-06	4.390E-06	4.495e-006	2.195e-006	1.610E-06		
4	7.195E-06	6.390E-06	6.495e-006	4.195e-006	1.610E-06		
5	9.195E-06	8.390E-06	8.495e-006	6.194e-006	1.610E-06		
6	1.120E-05	1.039E-05	1.050e-005	8.199e-006	1.610E-06		
7	1.370E-05	1.239E-05	1.300e-005	1.070e-005	2.610E-06		
8	1.720E-05	1.539E-05	1.650e-005	1.420e-005	3.610E-06		
9	2.170E-05	1.939E-05	2.100e-005	1.870e-005	4.610E-06		
10	2.770E-05	2.439E-05	2.700e-005	2.470e-005	6.610E-06		
11	3.520E-05	3.139E-05	3.450e-005	3.220e-005	7.610E-06		
12	4.420E-05	3.939E-05	4.350e-005	4.120e-005	9.610E-06		
13	5.570E-05	4.939E-05	5.500e-005	5.270e-005	1.261E-05		
14	7.020E-05	6.239E-05	6.950e-005	6.719e-005	1.561E-05		
15	8.870E-05	7.839E-05	8.800e-005	8.570e-005	2.061E-05		
16	1.122E-04	9.939E-05	1.115e-004	1.092e-004	2.561E-05		
17	1.412E-04	1.254E-04	1.405e-004	1.382e-004	3.161E-05		
18	1.782E-04	1.574E-04	1.775e-004	1.752e-004	4.161E-05		
19	2.247E-04	1.994E-04	2.240e-004	2.217e-004	5.061E-05		
20	2.827E-04	2.504E-04	2.820e-004	2.797e-004	6.461E-05		
21	3.562E-04	3.154E-04	3.555e-004	3.532e-004	8.161E-05		
22	4.487E-04	3.974E-04	4.480e-004	4.457e-004	1.026E-04		
23	5.652E-04	5.004E-04	5.645e-004	5.622e-004	1.296E-04		
24	7.117E-04	6.304E-04	7.110e-004	7.087e-004	1.626E-04		
25	8.962E-04	7.934E-04	8.955e-004	8.932e-004	2.056E-04		
26	1.229E-03	9.994E-04	1.228e-003	1.226e-003	2.586E-04		
27	1.421E-03	1.258E-03	1.420e-003	1.418e-003	3.256E-04		
28	1.789E-03	1.584E-03	1.788e-003	1.786e-003	4.096E-04		
29	2.253E-03	1.994E-03	2.252e-003	2.250e-003	5.166E-04		
30	2.836E-03	2.511E-03	2.835e-003	2.833e-003	6.496E-04		
31	3.571E-03	3.161E-03	3.570e-003	3.568e-003	8.186E-04		
32	4.496E-03	3.980E-03	4.495e-003	4.493e-003	1.031E-03		
33	5.811E-03	5.011E-03	5.810e-003	5.808e-003	1.600E-03		

Table 8. Gate specifications. Center times for both SLM and HM are shifted according to calibration time shift given in Table 10. Grey bars indicate the gates that are actually used for the data interpretation. The gates that are affected by the coil response –too much to be used for the interpretation- are shown as light-grey bars. Note that the earliest and latest gates actually used for each sub-area highly depend on the local resistivity values. Here it corresponds to one of the "best" area where the resistivity is very low and where a maximum number of gates can be used.

Parameter	SLM	HM	Noise
Front gate time	-	62.5E+6 s	-
Number of shoots per cycle	256	64	64
SLM + HM cycles between Noise Cycles	-	-	10
Gates measured	1-25	1-33	1-37
Gates used	7-25	15-33	1-33

Table 9. Receiver specifications.

4.4 Calibration of the SkyTEM system

Prior to the survey, the SkyTEM equipment was calibrated by SkyTEM Surveys ApS on the Danish national TEM test site near Aarhus, Denmark. The calibration is performed to establish the absolute time shift and data level in order to facilitate precise data modeling. No additional leveling, or drift corrections are applied subsequently.

In order to perform the calibration, all system parameters (transmitter waveform, low pass filers, etc.) must be known to allow modeling of the used SkyTEM configuration.

The calibration constants are determined by comparing a recorded SkyTEM response on the test site with the reference response. The reference response is calculated from the test site reference model for the used SkyTEM configuration. This procedure is repeated for a number of different attitudes.

Documentation of the calibration procedure can be found in Foged et al. (2013).

Moment	Time Shift	Scale Factor
SLM	-0.70 µs	0.92
HM	-3.00 µs	0.92

Table 10. Calibration constants with regards to the Danish national TEM test site reference model, 2011.

4.5 SkyTEM repeatability test

To monitor that there is no changes to the system during the mapping, repeated measurements are performed by hovering on a specific spot in the vicinity of the landing ground. This is done every time the helicopter takes off or returns from a flight.

4.6 High altitude test

A high altitude test was conducted near the test area to identify the system response. The test is performed by measuring at an altitude where the ground response is negligible. The documentation for the high altitude tests can be found in the SkyTEM Surveys ApS data acquisition report (SkyTEM, 2011).

4.7 Bias tests during production flight

Each production flight includes bias tests performed on the way to and from the production lines. Where cloudiness permitted, they were performed at altitudes of 300 m or more. The bias tests are similar to the high-altitude test and serve to identify changes in the system response between flights.

5. PROCESSING OF THE SKYTEM DATA

The software package Aarhus Workbench is used for the processing of the SkyTEM data.

The aim of processing is to prepare data for the geophysical interpretation. The processing primarily includes filtering and averaging of data as well as culling and discarding of distorted or noisy data. The data is stored in a database. The settings for the different processing steps are also stored.

Processing can be divided into four steps:

1. Import of raw data into a fixed database structure. The raw data appear in the form of .dat-, .sps- and .geo-files. Dat-files contain the actual transient data from the receiver. Sps-files contain GPS positions, tilts, altitudes, transmitter currents etc. and the geo-file contains system geometry, low-pass filters, calibration parameters, turn-on and turn-off ramps, calibration parameters, etc. For a description of the SkyTEM file formats see (HydroGeophysics Group 2011).
2. Automatic processing: First, an automatic processing of the four data types is used. These are GPS-, altitude-, tilt- and TEM data. This automatic processing is based on a number of criteria adjusted to the survey concerned.
3. Manual processing: Inspection and correction of the results of the automatic processing for the data types in question.
4. Adjustment of the data processing based on preliminary inversion results.

All data is recorded with a common time stamp. This time stamp is used as key when linking data from different data types. The time stamp is given as the GMT time.

In the following a short description of the processing of the different data types is shown. A more thorough description of the SkyTEM processing module of the Aarhus Workbench is found in (HydroGeophysics Group, 2011).

5.1 Positioning

The position of the frame is measured with two independent GPS receivers, which record data continuously with an uncertainty of ~3 m.

5.2 Tilt data

The roll and the pitch of the frame are measured and used to correct the altitude and voltage data. It is presumed that the frame is rigid so that the tilts of the transmitter and receiver are identical. During the processing, a running mean is calculated for the roll and the pitch.

5.3 Altitude data

The distance between the transmitter coil and the ground is measured with two independent lasers. Figure 5 shows an altitude data example over open country and a minor forest area.

The aim of the altitude data processing is to remove reflections that do not come from the ground - typically reflections from treetops. The processing is based on the fact that reflections from tree tops etc. result in an apparently lower altitude. Altitude processing is done using an algorithm that filters out data by repeatedly making a polynomial fit to the data while removing data that are some meters below this polynomial. Thereby reflections from treetops are removed. The automatic filtering is followed by a manual inspection and correction. In the end the individual soundings are assigned the correct elevation by using a dense Digital Elevation Model (DEM, here with a grid spacing of 10 m).

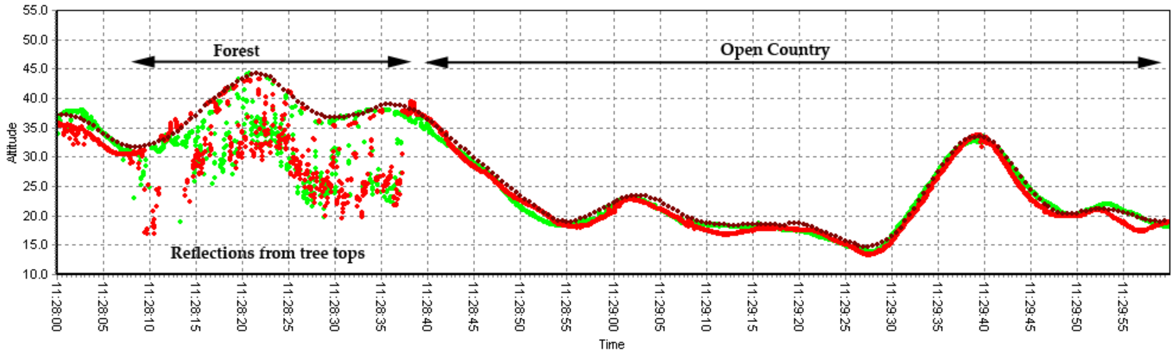

Figure 5. Green and red dots are raw data from the two laser altimeters. Brown dots are the resulting altitude after filtering the data. The time window holds approximate 2 km of data.

5.4 Voltage data

The Voltage data are gathered continuously along the flight lines and alternately with a low and a high moment. The processing of voltage data is done in a two-step system: an automatic and a manual part. In the former, data are corrected for the transmitter/receiver tilt, and a number of filters designed to cull coupled or noise influenced data are deployed. Furthermore, data are averaged to increase the signal-to-noise ratio using a trapezoidal averaging core, where the averaging width of late-time data is larger than that of early-time data, as seen in Figure 7. The data uncertainty is calculated from the data stack. Furthermore, a small uniform data uncertainty of 3% is assigned to all data. Soundings are typically taken out for every 20-30 m depending on flight speed, SkyTEM-setup and target. In the present survey the raw soundings are spaced by about 15 m. The average soundings have the same spacing, but the final lateral resolution of the top 30 m is more likely about 30-50 m depending on the ground resistivity due to the lateral integration of the transmitter loop and to the diffusivity of the EM field.

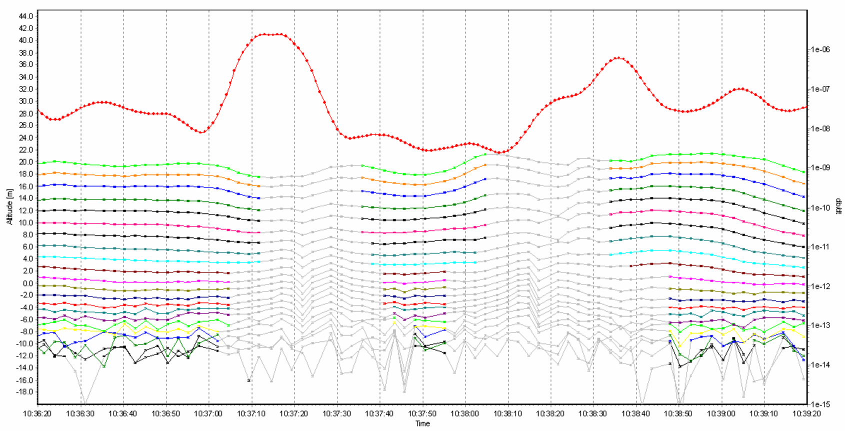

Figure 6. The section displays 3 minutes (~2.2 km) of data. The upper red curve shows the flight altitude. Each of the lower curves shows raw high-moment data for a given gate time. The green line represents gate 1 of the high moment, the orange line gate 2 etc. The grey lines represent data that have been removed due to couplings. Two couplings can clearly be spotted at 10:37:20 and 10:38:20. Comparing these spots with a map, it is seen that both couplings have been associated with installations along roads. The couplings here particularly affect the late-time signal (the lower curves).

After the automatic processing, soundings are inspected visually using a number of different data plots. At this stage, it is assessed whether data points should be ascribed a higher uncertainty or removed entirely. The evaluation is done by looking at the decay curves, the distance to potential noise sources and the noise measurements. Survey areas are typically crossed by a number of power lines, roads and railroads. As data near such installations often couple to the installations, it is necessary to inspect all data and remove coupled data when found, in order to produce geophysical maps without the influence of manmade installations. In some cases it is not possible to identify the source of the coupling even though data clearly show that there must be a source. Figure 6 shows an example of strongly coupled data near two roads. When the couplings have been removed, the data are stacked into soundings. The stacked data are then inspected to exclude the part of the late-time data where the background noise level reaches the level of the earth response.

For a description on noise contamination in electromagnetic data, see (Munkholm and Auken, 1996).

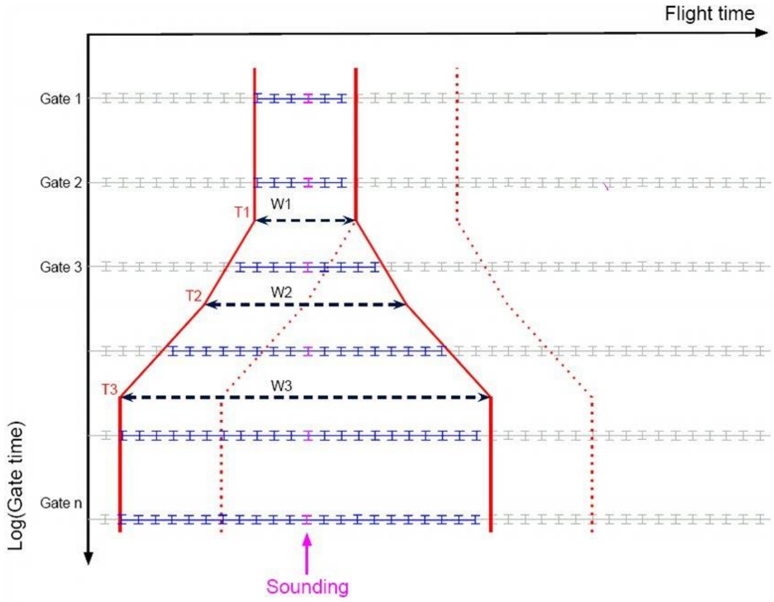

Figure 7. Trapezoid averaging of TEM-data. The raw data series within the red lines (blue points/error bars) are averaged yielding the sounding marked by violet points/error bars. The averaging trapezoid is subsequently moved (red dashed line), and a new sounding is created. The times T1-3 and widths W1-3 define the trapezoid.

5.5 Processing - Technical specifications

Table 11 shows the processing settings used in the Aarhus Workbench.

Note that a new set of trapezoid filter has been introduced in Aarhus Workbench. This second set is normally deactivated by default, but can be activated to apply different filter widths above a given altitude. The purpose is to narrow the filters as much as possible, especially for early gates where the signal-to-noise is quite strong, in order to improve the lateral resolution of the near surface. This is because the amplitude of the earth signal is mainly depending on the flight altitude, the signal being lower with the increase of the altitude. Of course the ground resistivity has also an impact on the earth signal, this last one becoming stronger with the decrease of the resistivity. However, the resistivity over the present survey area is relatively homogeneous, there are no big lateral resistivity contrasts. Then the altitude parameter is mainly responsible for the earth signal level variations.

One can note in Table 11 that only widths of the SLM, where early gates are present, have been set to two different groups of values. Changing HM parameters would not have been worthy.

Item		Value
Software	Aarhus Workbench Version	4.0
Noise Processing	Data uncertainty: Uniform data STD	Estimated from data stack 3%
Trapezoid filter	Sounding distance SLM, times: T1, T2, T3 [s] SLM, width: W1, W2, W3 [s] HM, times: T1, T2, T3 [s] HM, width: W1, W2, W3 [s]	1.5s (~15 m) 1e-5, 1e-4, 1e-3 6, 8, 12 1e-5, 1e-4, 1e-3 6, 12, 20

Table 11. Processing settings (See Figure 7 for Trapezoid filter description).

6. INVERSION OF THE SKYTEM DATA

Inversion and evaluation of the inversion result are done using the Aarhus Workbench software package. The underlying inversion code is developed by the HydroGeophysics Group, Aarhus University, Denmark (Christansen et al., 2011).

6.1 Coil response inversion

The information about the near-surface geology is contained in the early part of the sounding curve. In order to improve the resolution of the near-surface geology, it is important to be able to obtain useful data as early as possible on the sounding curve. The signal from the very early times also contains a signal from the instrument itself. This interfering signal is called the coil response as it is caused by the coupling of the primary field to the receiver coil. Normally, gates are discarded where the coil response is more than about 5% of the measured signal. Usually, this means that only gates from approximately 11-12 μs after turn-off can be used. With the coil response inversion concept, the signal is adaptively compensated for the coil response signal so that the coil response affected gates in the interval 7-11 μs may also be included in the interpretation. This, however, requires that SkyTEM mapping is collected with an optimized SkyTEM setup with sufficient gates in the part of the sounding curve where the coil response signal can be determined.

The size of the coil response signal is determined by making measurements at high altitude (> 600 m). Here the signal from the ground makes out just a tiny proportion of the measured signal, which instead is dominated by random background noise and coil response. If data are averaged, the random background noise will be stacked out, and the coil response signal can be quantified. This principle is illustrated in Figure 8. The grey and blue lines show data from high altitude means over soundings from time intervals of 6 s (grey line) and 768 s (blue line). The two green lines illustrate how the background noise is effectively decreased by a factor of about 10 (approximately the square root of 6/768) due to averaging. The red circles show the gates that are not diminished by averaging since they are dominated by the coil response signal. The coil response signal can be assumed to be exponentially decaying, as shown with the red slash through the red circles in Figure 8B. Also plotted on the figure are two (green) curves showing the typical level of the measured signals at 30 m (top) and 40 m (bottom) altitude, respectively.

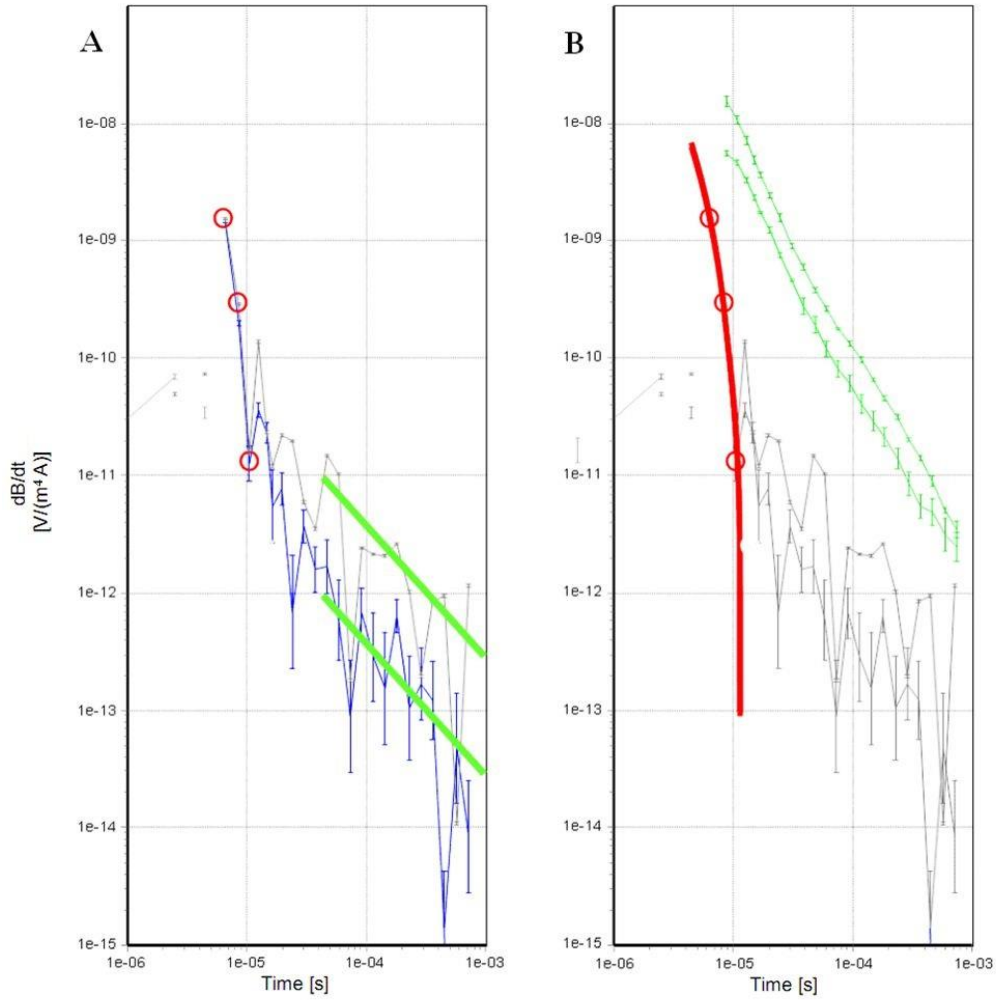

Figure 8: The figure illustrates the principle for coil response correction. A: Stacked SLM data from high altitude. The stacks of 6 s and 768 s, respectively, are shown as a grey and a blue line. The green lines show how the background noise is decreased by a factor of about 10 from averaging over longer time intervals. The red circles show gates that are virtually unchanged since the coil response signal dominates the background noise. B: Stacked SLM data from high altitude. The red line shows the coil response signal. The green lines show the level of a typical measured signal from 30 m (top) and 40 m (bottom) altitude, respectively. The first gate of the measured signal at 40 m contains about 8% coil response signal and is clearly dragged down by a, in this case, negative coil response signal.

The coil response signal is not constant for a full survey. There may be slight variations in the level during each flight, and the level can also be displaced if the receiver coil is repositioned a few millimeters due to a hard landing. The shape of the coil response signal, however, is assumed to be constant. With this in mind, the coil response signal simply cannot be subtracted from the measured signal and applied to the early time gates. Instead, a coil response function is introduced with the coil response inversion concept which, during the inversion, adaptively compensates for the coil response. This is illustrated in Figure 9. Inversion with coil response correction is progressing similar to the normal inversion. The total forward response, consisting of the normal forward responses plus a contribution from the coil response function, is compared with the measured signal. Small adjustments of the inversion parameters and the level of coil response function are performed before the next comparison. This continues until the total forward response is sufficiently close to the measured signal to consider the inversion completed.

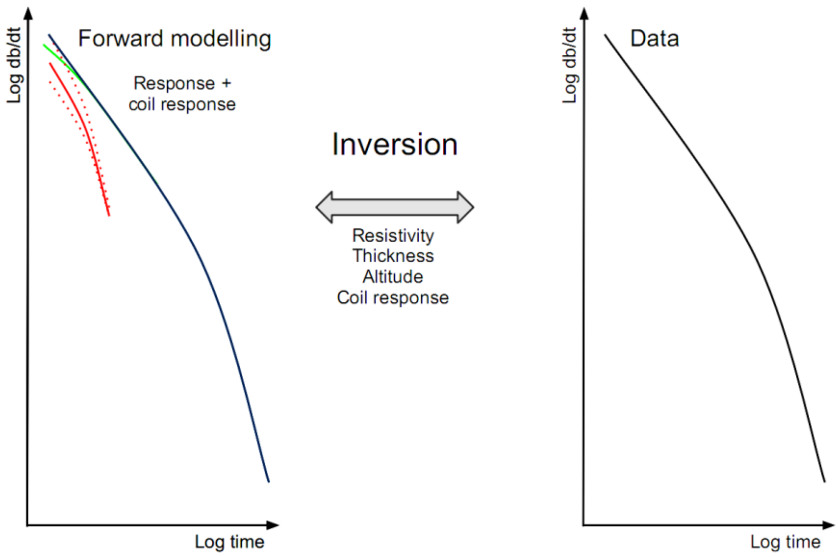

Figure 9. Inversion with coil response correction. The total forward response (blue curve) consisting of the normal forward response (green curve) plus a contribution from the coil response function (red curve), is compared to the measured signal (black curve). Small adjustments of the inversion parameters (that determine the normal forward response) and the level of the coil response function are performed before the each comparison until the total forward response is sufficiently close to the measured signal.

The coil response function is introduced based on the following assumptions:

- The shape of the coil response function is fixed and identical to the coil response signal at high altitude. The level of coil response function is variable.
- Major variations in the level of coil response function from flight line to flight line can occur.
- Only minor variations in the level of coil response function from sounding to sounding is present.

Within the Aarhus Workbench those assumptions can be applied by using coil response settings that a) sets the level of the coil response with a loose prior constraint to the level of the high altitude test and b) sets a tight lateral constraint to the level of the coil response along the flight line. If the inversion needs to shift the level of the coil response function along an entire flight line, it can do so as long as the level from sounding to sounding does not change too much.

6.2 Spatially constrained inversion

The spatially constrained inversion (SCI) uses constraints between the 1D-models, both along and across the flight lines, as shown in Figure 10. The inversion is a 1D full non-linear damped least-squares solution in which the transfer function of the instrumentation is modeled. The transfer function includes turn-on and turn-off ramps, front gate, low-pass filters, and transmitter and receiver positions. The flight altitude contributes to the inversion scheme as a model parameter with the laser altimeter readings as a constrained prior value.

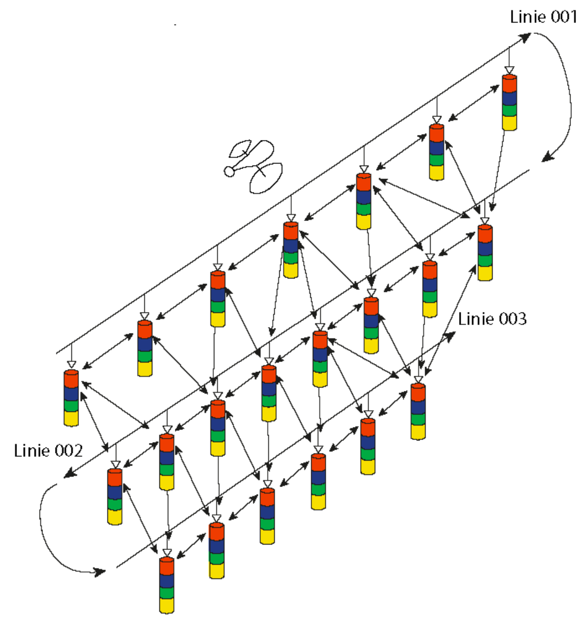

Figure 10. Schematic presentation of the SCI concept. Constraints connect not only soundings located along the flight line, but also those across them.

In the SCI scheme, the model parameters are tied together with a spatially dependent covariance scaled according to the distance between soundings. The constraints between the soundings are designed using Delaunay triangles, also called nearest neighbors (see Figure 11). In this way each sounding is linked to its "best companions". For Airborne EM surveys, Delaunay triangulation always connects a sounding to its two nearest soundings along the flight line and one or more soundings on each of the adjacent flight lines, which is the preliminary condition for breaking down the line orientation in the data.

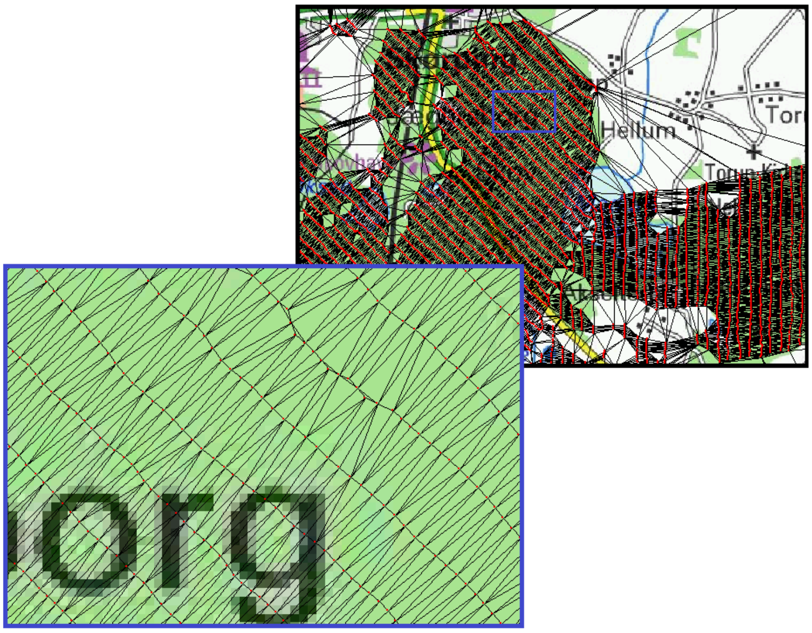

Figure 11. Example of setup of SCI-constraints. The red points are the sounding positions. The black lines show the constraints created with the Delaunay triangles. The line distance in this example is 160 m and the zoomed area is approximately 1.2 x 0.85 km large

In addition to constraints on model parameters (resistivites, layer interfaces), there are also lateral constraints on the altitude, however, only along the flight line.

Constraining the parameters enhances the resolution of resistivities and layer interfaces which are not well resolved in an independent inversion of the soundings.

Until recently, un order to perform the SCI in a CPU efficient manner, a typical data set of thousands of soundings had to be divided into smaller subsets. Each subset was then inverted with spatial constraints, as a unit. We produced the cells using the preconstructed Delaunay triangles, normally up to a size of 4000 model parameters. To ensure continuity over the cell boundaries, soundings on the boundaries were inverted in both cells in the first inversion step. The average of the boundary models from the two cells were used as prior model for the final inversion step. For this survey report a new enhanced version of the inversion program, AarhusInv, was used to make single-cell SCIs, avoiding the step of averaging at cells' boundaries.

The SCI inversion scheme is developed for parameterized inversion with normally 4 or 5 layers and for smooth inversion with e.g. 20 layers, each having a fixed thickness, but a free resistivity. Vertical constraints are applied to the smooth models to stabilize the inversion. Both schemes have advantages. Layer interfaces and resistivities are best determined from the parameterized inversion. On the other hand, smooth inversion is more independent of the starting model, and gradual transitions in resistivities are more conspicuous facilitating the delineation of complex geological structures. Further details about the SCI-inversion scheme can be found in (HydroGeophysics Group, 2008) and (Viezzoli et al., 2008).

The SCI-setup parameters for this survey are listed in section 6.4.

6.3 Depth of Investigation (DOI)

A concept of estimating the depth of investigation (DOI) (Christiansen and Auken, 2010) for the individual models has been applied with this survey. The DOI calculation takes into account the SkyTEM system transfer function, the number of data points, and the data uncertainty.

EM fields are diffusive, and there is no specific depth below which there is no information on the resistivity structure. Therefore, always two numbers are presented for the DOI – an upper and a lower number. As a guideline the layers above DOI upper are well founded in data. Between DOI upper and DOI lower the model is not as strong in the data, and below DOI lower the model is very weak in the data, and interpreting these parts of the model should be done with utmost caution.

DOI – technical description
Depth of investigation (DOI) is a useful tool for evaluation of inversion results and holds useful information when a geological interpretation is made. However, for diffusive methods, such as ground based or airborne EM, there is no specific depth below which there is no information on the resistivity structure. The question is to which depth the model is most reliable.

The DOI-method used by Aarhus Workbench is based on the actual inverted model, and it includes the full system transfer function and system geometry, using all actually measured data and their uncertainties. The methodology is based on a recalculated sensitivity (Jacobian) matrix of the final model. A priori information, model constraints or other information added to the system are not considered. Thus, the DOI is purely data driven.

To demonstrate the methodology, an example with a SkyTEM set-up with the last gate at 3 ms is used. Assuming a simple 3-layer model, the sensitivity function can be plotted versus depth (left image in Figure 12). The sensitivity function comes directly from the recalculated sensitivity matrix (Jacobian). As expected, the sensitivity to the second layer is low whereas there are high sensitivities to the first and the third layers.

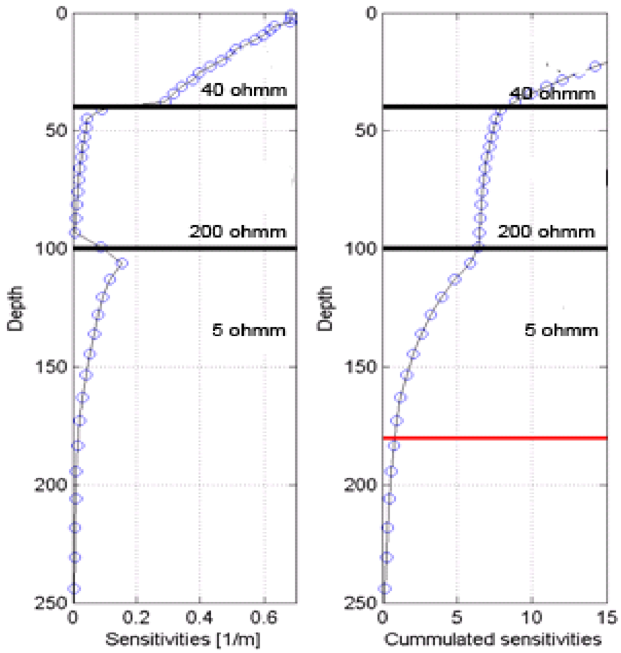

Figure 12. Sensitivities calculated for a rediscretized version of the model indicated by the black lines; resistivities of layers are written on the plot. The left plot is the sensitivity function itself. The right plot shows the cumulated sensitivities. The red line indicates the DOI given by the global threshold value.

If the sensitivities are summed up from deep to shallow, the right side image in Figure 12 emerges. This plot shows the total sensitivity in a given depth and downwards. Next, a threshold value that indicates the minimum amount of sensitivity needed for indicative information is set. In the example in Figure 12, a threshold value of 0.8 was settled upon, giving a DOI of approximately 180 m.

Setting the threshold value is very much a question of tuning based on experience and comparing different models with different methods. The threshold value used here has been tested on many different models and with different systems and produces trustworthy results in all cases.

In this case the model was sub-discretized into many layers to support the visual understanding of the concept. In fact, it is not necessary to sub-discretize a model with few layers into more than maybe 12-15 layers to obtain a reasonably precise DOI - e.g. within 3-5 m for the examples in Figure 12.

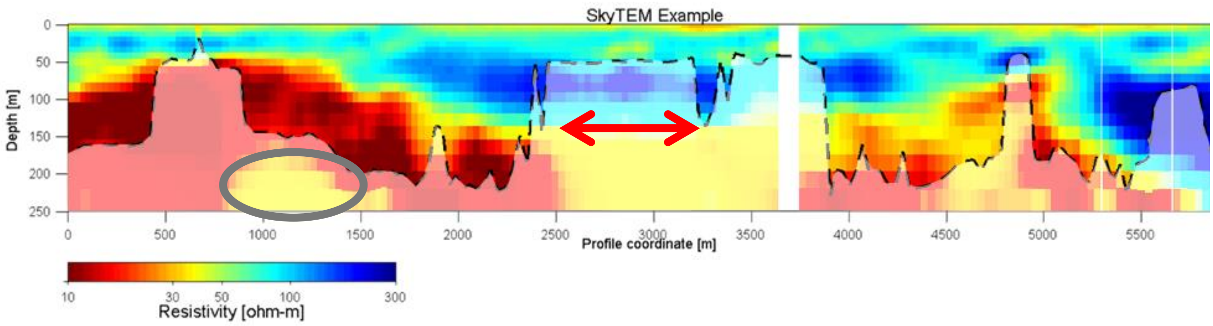

Figure 13. SkyTEM resistivity section example with DOI shown as a black dashed line. In the area marked with a grey circle, the DOI indicates that there is no information on the less conductive structure. The red arrow marks an area where the high-moment data are missing, which results in a shallower DOI.

The DOI is purely data driven, which means that information above the DOI is data controlled whereas the information below the DOI is mainly controlled by the inversion settings, such as starting model, lateral and vertical constraints. Thus, sometimes the DOI is well above the deepest layers. Figure 13 shows a smooth inversion of SkyTEM data from Denmark; the black dashed line indicates the DOI. In the area marked with the grey circle, the DOI indicates that data have no information on that less conductive structure. The arrow indicates an area where the high-moment data are missing, which means a shallower DOI. The effect of the constraints is clearly seen as the high-resistive layer is nicely pulled through to create a geologically reasonable interpretation. This is exactly one of the main functions of the constraints - they are user defined numbers for the geological homogeneity and thus ensure model smoothness even in areas with limited information from the data themselves.

6.4 Inversion - Technical specifications

The inversion settings used for the smooth inversion in the Aarhus Workbench are listed below.

Item		Value
Software	Aarhus Workbench Version	4.0
SCI cells	Approximate cell size [number of models]	Single section SCI*
Starting model	Number of layers Starting resistivities [Ωm] Thickness of first layer [m] Depth to last layer [m] Thickness distribution of layers	29 AutoRes** 4.0*** 650.0 Log increasing with depth
SCI constraint/ Prior constraint	Horizontal constraints on resistivities [factor] Reference distance [m] Constraints distance scaling Vertical constraints on resistivities [factor] Prior, thickness Prior, resistivities Prior on flight altitude [m] Lateral constraints on flight altitude [factor] Minimum number of gates per moment	1.35 20 (1/distance) 3.0 Fixed None +/- 0.5 **** 1.3 7

*Table 12. Inversion settings, smooth SCI setup.*Except for the Taylor Valley area for which the usual cell size of 100 has been used (problem of convergence when inverting with one big cell), all sub-areas have been inverted with one single cell, which avoids to make a 2nd run during the SCI for averaging the boundaries between the cells. **A homogeneous starting resistivity is dynamically evaluated at each sounding location by a direct transform from the db/dt curves, this helps to better handle strong lateral resistivity variations within a same area. ***The thickness of the first layer has been set to 1.5m for hyper-saline Vida and Vanda Lakes, the resistivity variations being essentially in the near surface for these sub-areas.****The altitude can be set quite tight for this Antarctica survey as there is no vegetation. Also due to the very high top resistivity in many places, the inversion can easily change the altitude to compensate a first very resistive layer, which means that a tight a priori constraint is really recommended.*

7. THEMATIC MAPS AND CROSS SECTIONS

To visualize the resistivity structures in the mapping area, a number of geophysical maps and cross sections have been created from the smooth inversion results by using the Aarhus Workbench. Furthermore, a location map and a number of maps made for quality control (QC-maps) are found in the appendices. The Aarhus Workbench Workspace that holds the inversion results including mean resistivity maps, cross sections, etc. can, upon request, be delivered.

7.1 Mean resistivity maps

The inversion result consists of a large number of 1D-models described by depth intervals (i.e. layers) and resistivities within each model. These are then normally used to calculate mean resistivities to obtain a visualization of the resistivity distribution in the mapping area. Figure 14 shows how the resistivities of the layers in a model influence the calculation of the mean resistivity in a depth interval [A, B]. d_0 is the surface, d_1, d_2 and d_3 are the depths to the layer boundaries in the model. ρ_1, ρ_2, ρ_3 and ρ_4 are the resistivities of the layers.

The model is subdivided into sub-thicknesses $\Delta t_{1\text{-}3}$. The mean resistivity ($\rho_{vertical}$) is calculated as:

$$\rho_{vertial} = \frac{\rho_1 \cdot \Delta t_1 + \rho_2 \cdot \Delta t_2 + \rho_3 \cdot \Delta t_3}{\Delta t_1 + \Delta t_2 + \Delta t_3}$$

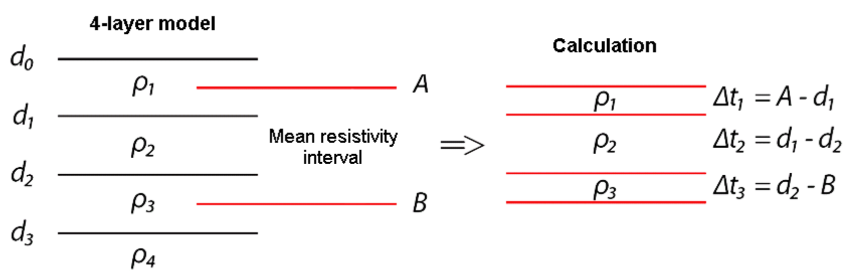

Figure 14. The figure illustrates how the resistivities of the layers influence the mean resistivities in a depth interval [A:B]

In the general term the mean resistivities in a depth interval is calculated using the equation below:

$$\bar{\rho} = \frac{\sum_{i=1}^{n} \rho_i \cdot \Delta t_i}{\sum_{i=1}^{n} \Delta t_i}$$

where *i* runs through the interval from 1 to the number of sub-thicknesses. The mean resistivity calculated by the above formula (ρ_{vertical}) is named the vertical mean resistivity - equal to the total resistance if a current flows vertically through the interval.

By mapping with the TEM method, the current flows only horizontally in the ground. Therefore, the mean resistivity is calculated as if the current runs horizontally in the interval. This resistance is described as the horizontal mean resistance ($\rho_{\text{horizontal}}$) and is the reciprocal of the mean conductivity (σ_{mean}).

The horizontal mean resistivity is calculated in the following way:

$$\rho_{horizontal} = \frac{1}{\sigma_{mean}} = \left[\frac{\sum_{1=1}^{n}\left(\frac{1}{\rho_i}\right) \cdot \Delta t_i}{\sum_{i=1}^{n} \Delta t_i}\right]^{-1}$$

Normally, there is no major difference in the maps of mean resistivities calculated in the two different ways. The horizontal mean resistivity weights the low resistivities more than the vertical mean resistivities in exactly the same way as the TEM-method does.

For this mapping, horizontal mean resistivity themes have been generated from the smooth model inversion in two sets. Depth and elevation slices are all 5 m thickness (note that the vertical resolution of TEM results is still decaying with depth).For this mapping the DOI has been used to blind resistivities of models below the DOI lower. The generated themes, consisting of mean resistivity values at each sounding position, are then gridded using the Kriging (Pebesma and Wesseling, 1998) method, with a node spacing of 30 m and a search radius of 200 m, to obtain a regular grid of resistivities.

Cross sections

The cross section shows a slice through a 3D-mean resistivity grid. The 3D-mean resistivity grid is interpolated from the 2D-mean resistivity grids based on the smooth model inversion result. The calculation of the 3D-grid from the stacked 2D-grids is illustrated in Figure 15.

a) For each 2D-mean resistivity grid, values are interpolated for a regular sampling along the profile.
b) The interpolation is repeated for all 2D-mean resistivity grids, creating a cross section grid.
c) Smoothing of the cross section grid is done by triangulation between the grid nodes.
d) The cross section is then colorized and the colors are faded in two steps below the DOI upper and the DOI lower values. Grey lines showing the DOI upper and DOI lower values gridded from models within 150 m are also plotted. This indicates the parts along the cross section that are most strongly founded in the data.

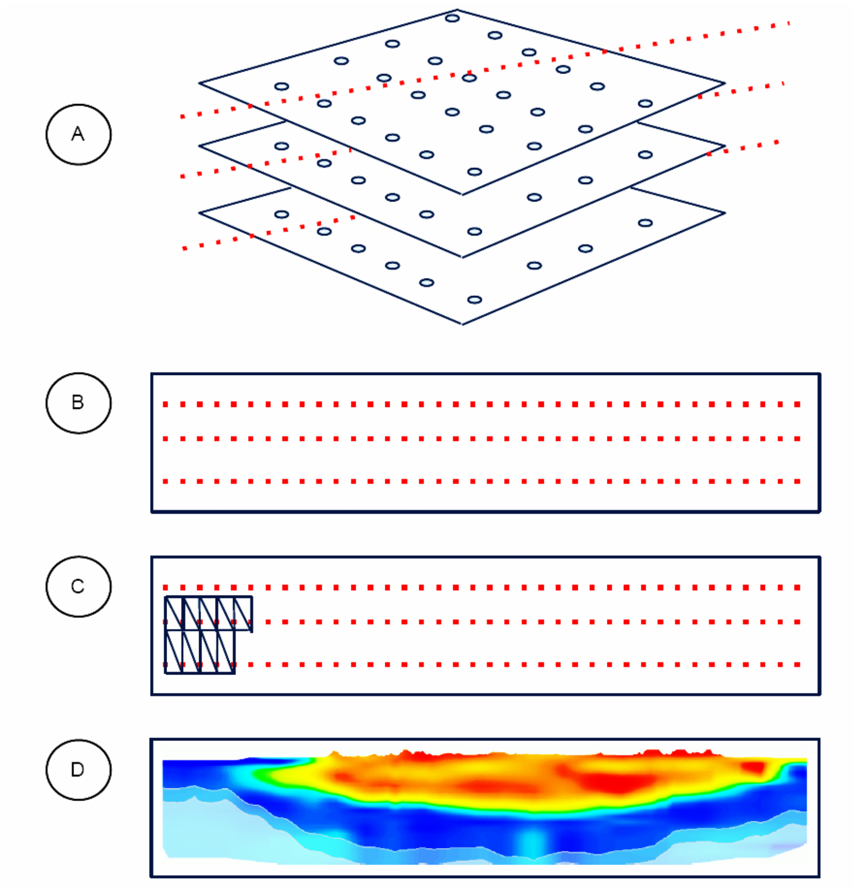

Figure 15. 3D grid interpolation. A) For each 2D-mean resistivity grid, values are interpolated for a regular sampling along the profile. B) The resulting cross section grid. C) Smoothing of cross section grid by triangulation. D) The resulting colorized cross section with the colors faded in two steps below the DOI upper and the DOI lower limits.

7.2 Location map, QC-maps

The maps listed below are included in **Appendix I**: The first and second sets correspond to Norsminde and Lillebæk areas, respectively.

Model locations and flight lines
This map shows the flight line positions overlaid by the model positions. Where no models are present, data has been discarded due to coupling. Line turns and some non-production intervals are also marked as discarded data. The couplings are mainly associated with major roads and power lines.

Moment indications
This map show the moments (low/high) present in each model. Both moments are presents in areas with low resistivity values from the top. If only deep conductor exists, it generally ends in the presence of the HM only, no conductor being present to produce TEM response at early and intermediate gates of the SLM. Where the ground is very resistive (>1000 Ωm), only few gates in the HM remain in the best scenario.

Flight altitude
This map shows the processed flight altitudes (heights) from the laser altimeters. The flight altitude of Antarctica survey, if not perturbed by the presence of forests or man-made installation, still increases in places where the helicopter has to fly above very steep slope and it is doing maneuvers. Otherwise, the nominal flight is about 30 m.

Data residual
This map shows the data residual (the data fit) for the individual models of the smooth model inversion. The data residual is normalized with the data standard deviation, so a data residual below one correspond to a fit within the data standard deviation. In general the data residual is low (below one). In Antarctica survey local high residuals are principally correlated with high resistivity values which provides very weak TEM signal close to noise level.

Depth of investigation (DOI) as depth

This map shows the DOI lower (in elevation) from the smooth model inversion (see section 6.3 for a description of the DOI-calculation). The DOI lower varies considerably over the survey area mainly due to hydrology and geology. For the present survey the DOI can be as small as 40 m in the most saline areas and as large as 400 m where the ice cover is very thick (Taylor Glacier).

8. CONCLUSION

The data has carefully been processed and interpreted to produce resistivity models with information down to a depth of 350 m.The results provide a new insight in the hydrogeological setting of the area.

The reader is referred to Mikucki et al., 2015 for the final results the hydrogeological interpretation of data.

9. REFERENCES

Christiansen, A. V. and Auken, E., 2010, A Global Measure for Depth of Investigation, Proceedings of the EAGE-NS, Zurich.

Christiansen, A. V., Auken, E., Foged, N., and Sørensen, K. I., 2011, Em1dinv - User manual. www.hgg.au.dk

Effersø, F., Auken, E. and Sørensen, K., 1999, Inversion of band-limited TEM responses. Geophysical Prospecting, 47, 551-564.

Foged, N., Auken, E., Christiansen, A.V., and Sørensen, K.I., 2013, Test-site calibration and validation of airborne and ground-based TEM systems: Geophysics, v. 78, no. 2, p. E95–E106, doi: 10.1190/geo2012-0244.1.

GFS, 2011, Refinement of the TEM reference model at Lyngby, www.gfs.au.dk.

HydroGeophysics Group, 2008, Spatially Constrained Inversion of SkyTEM data, Concept and Examples, www.hgg.geo.au.dk

HydroGeophysics Group, 2011, Guideline and standards for skytem measurements,processing and inversion, www.hgg.au.dk

Jørgensen, F., Lykke-Andersen, H., Sandersen, P., Auken, E. and Nørmark, E., 2003, Geophysical investigations of buried Quaternary valleys in Denmark: An integrated application of transient electro-magnetic soundings, reflection seismic surveys and exploratory drill-ings: Journal of Applied Geophysics, 53, 215-228.

Jørgensen, F., Sandersen, P. and Auken, E., 2003, Imaging buried Qua-ternary valleys using the transient electromagnetic method: Journal of Applied Geophysics, 53, 199-213.

Mikucki, J. A., Auken, E., Tulaczyk, S., Virginia, R.A., Schamper, S. Sørensen, K.I, Doran, P.T., Dugan, H. and N. Foley, 2015, Deep groundwater and potential subsurface habitats beneath an Anartic dry valley: Nature communications, 5:5831, doi: 10.1038/ncomms7831.

Munkholm, M.S. and Auken, E., 1996, Electromagnetic noise contam-ination on transient electromagnetic soundings in culturally disturbed environments. Journal of Environmental & Engineering Geophysics, Vol. 1, Issue 2, 119-127.

Nabighian, M. N. and Macnae, J. C., Time Domain Electromagnetic Prospecting Methods. In Nabighian, M. N. (editor), 1991, Electromagnetic Methods in Applied Geophysics, Vol. 2, Application, Part A, SEG.

Pebesma, E. J. and Wesseling, C. G., 1998, Gstat: A Program for geostatistical Modelling, Prediction and Simultation: Computers & Geosciences, 24, 17-31.

Sab, G.-A., 2012, Data processing of an Airborne Electromagnetic survey in Antarctica. Master thesis made at the Hydrogeogphysics Group, Aarhus University, Denmark.

SkyTEM ApS, 2011, SkyTEM Survey Alkmaar - Netherlands, Data acquisition report.

Sørensen, K. and Auken, E., 2004, SkyTEM - a new high-resolution helicopter transient electromagnetic system: Exploration Geophysics, 35, 191-199.

Viezzoli, A., Christiansen, A. V., Auken, E., and Sørensen, K. I., 2008, Quasi-3D-modeling of airborne TEM data by Spatially Constrained Inversion: Geophysics, 73, F105-F113.

APPENDIX I: LOCATION MAPS, QC MAPS

This appendix shows maps of:

- Model locations and flight lines
- Moment indications
- Flight altitude
- Data residual
- Depth of investigation as depth

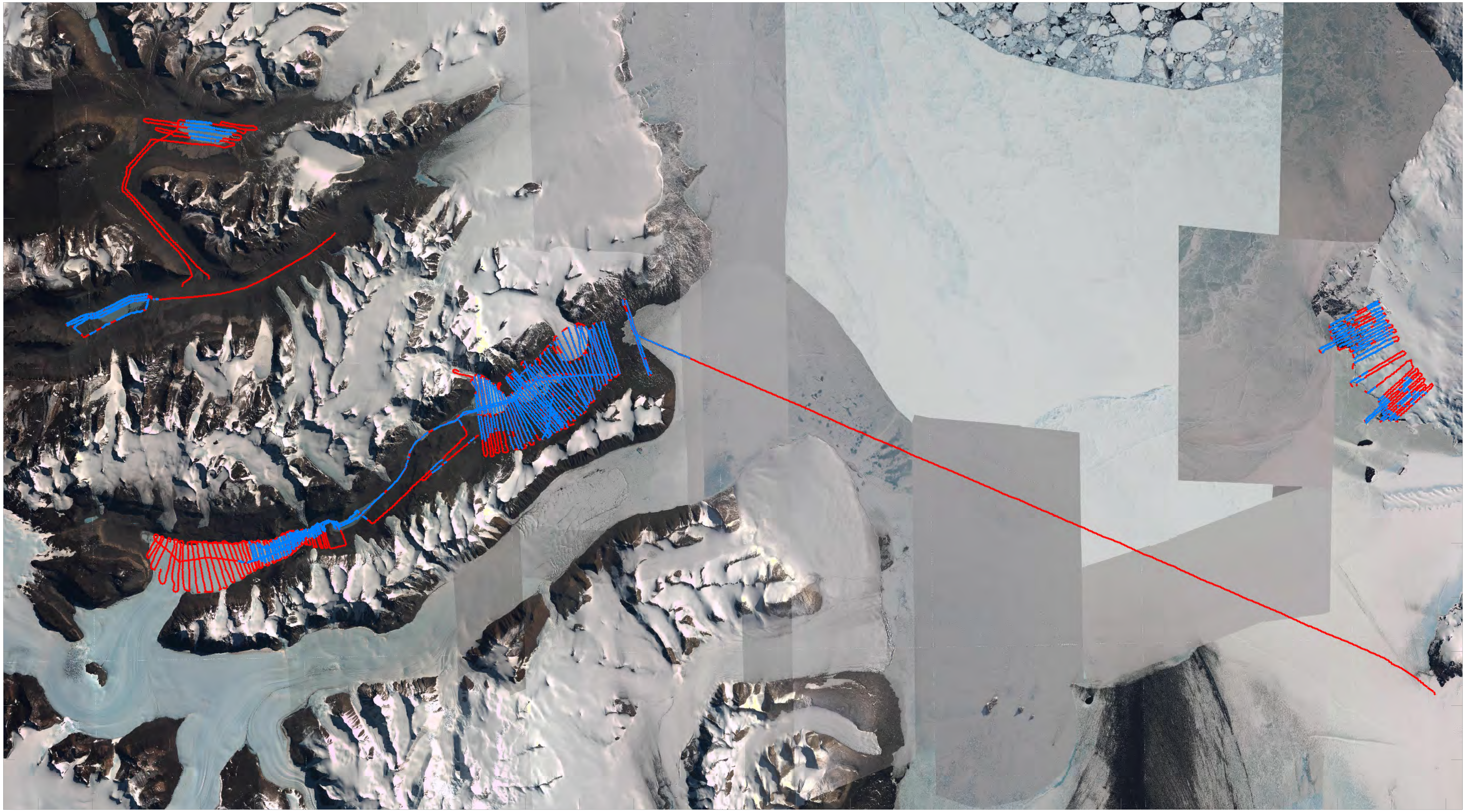

SkyTEM Survey Antartica		Location, flight lines
HydroGeophysics Group AARHUS UNIVERSITY	40 km UTM Zone 58S WGS84	Discarded data 1D model

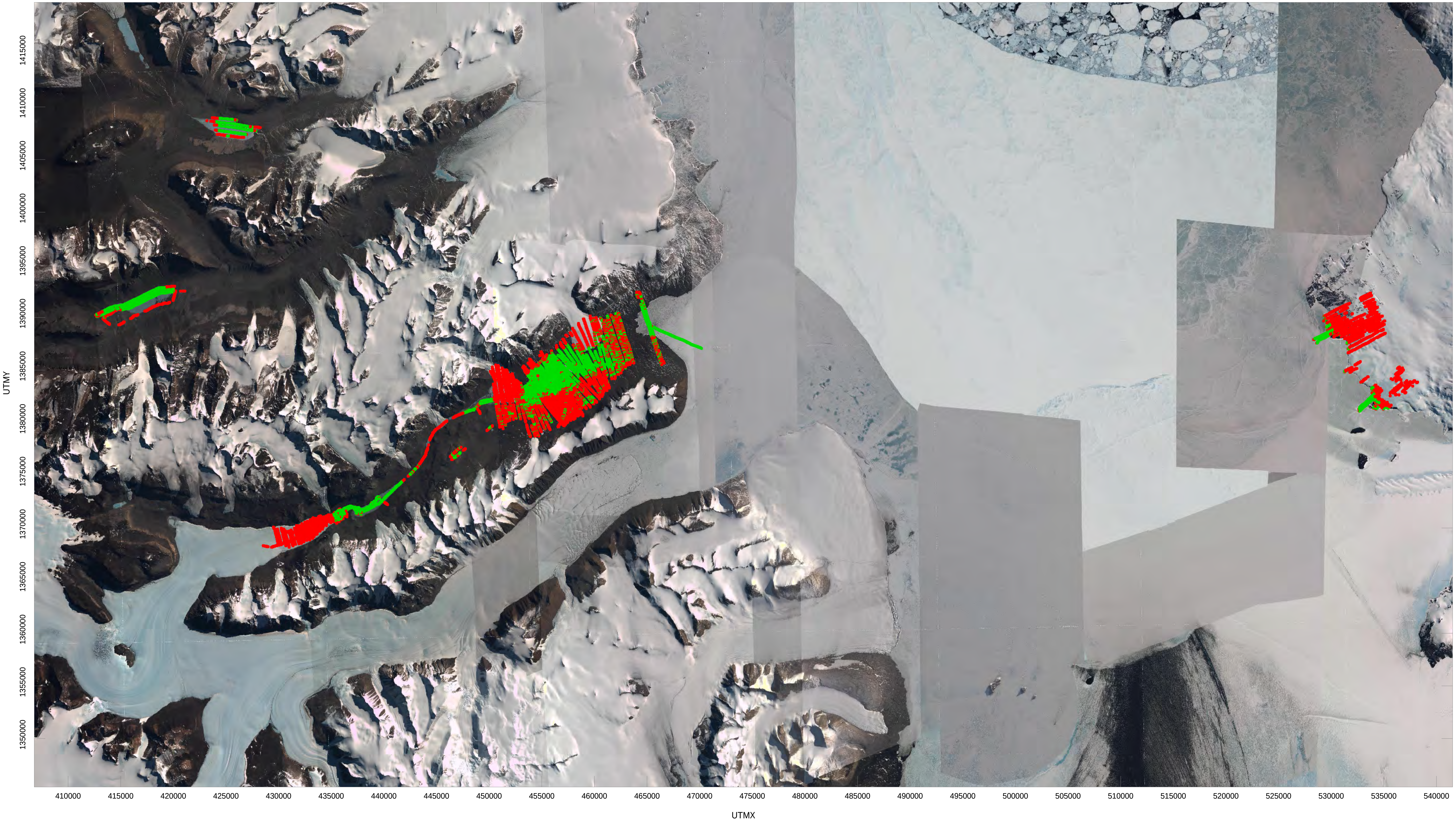

SkyTEM Survey Antartica		Moment Indications
HydroGeophysics Group AARHUS UNIVERSITY	40 km UTM Zone 58S WGS84	Models with both low and high moment data Models with only high moment data Models with only low moment data

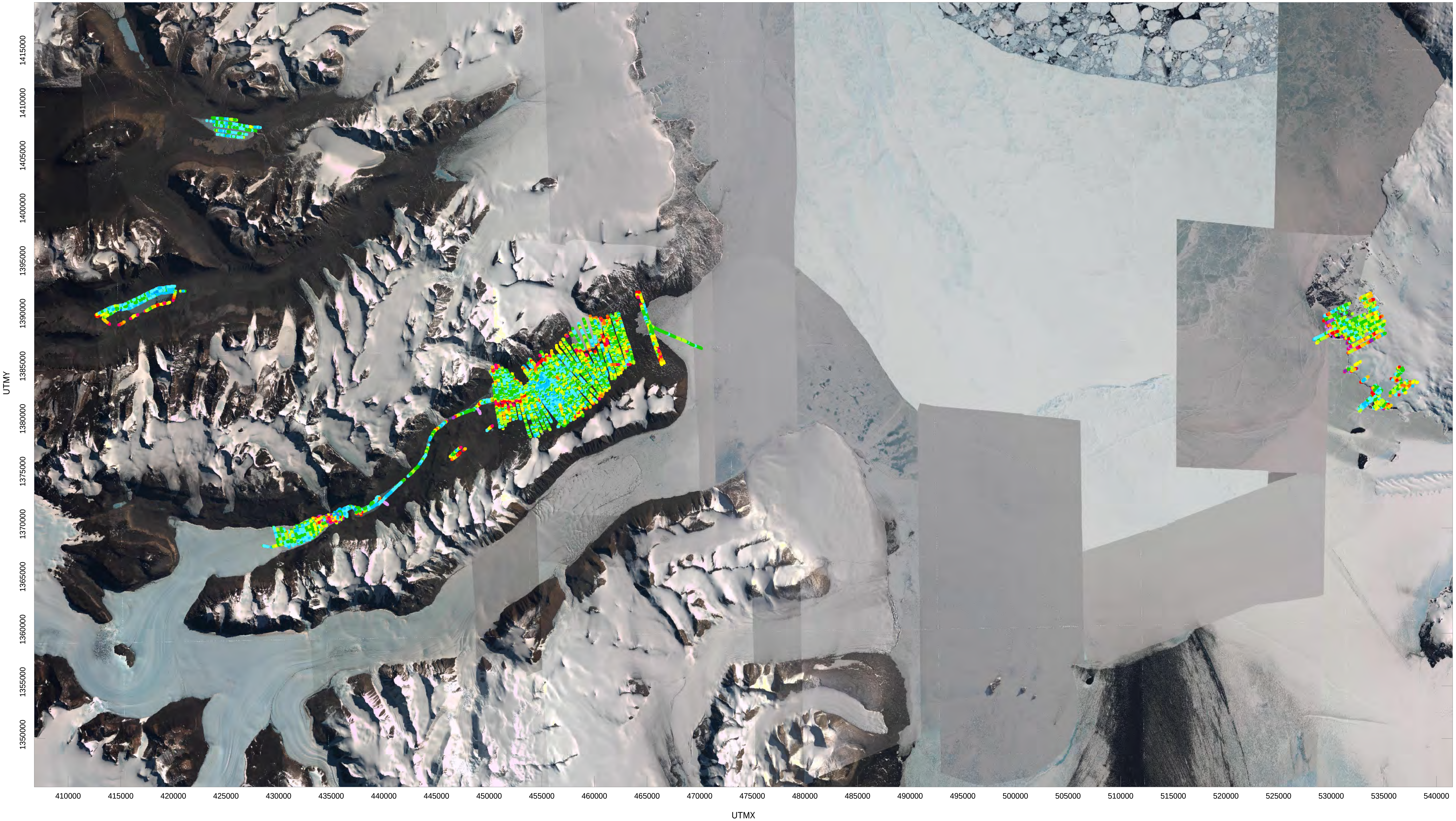

SkyTEM Survey Antartica

Flight Altitude

HydroGeophysics Group
AARHUS UNIVERSITY

40 km

UTM Zone 58S WGS84

10 15 20 25 30 35 40 45 50 55 60 65 70 75 80 85 90 95 100

Fligth Altitude [m]

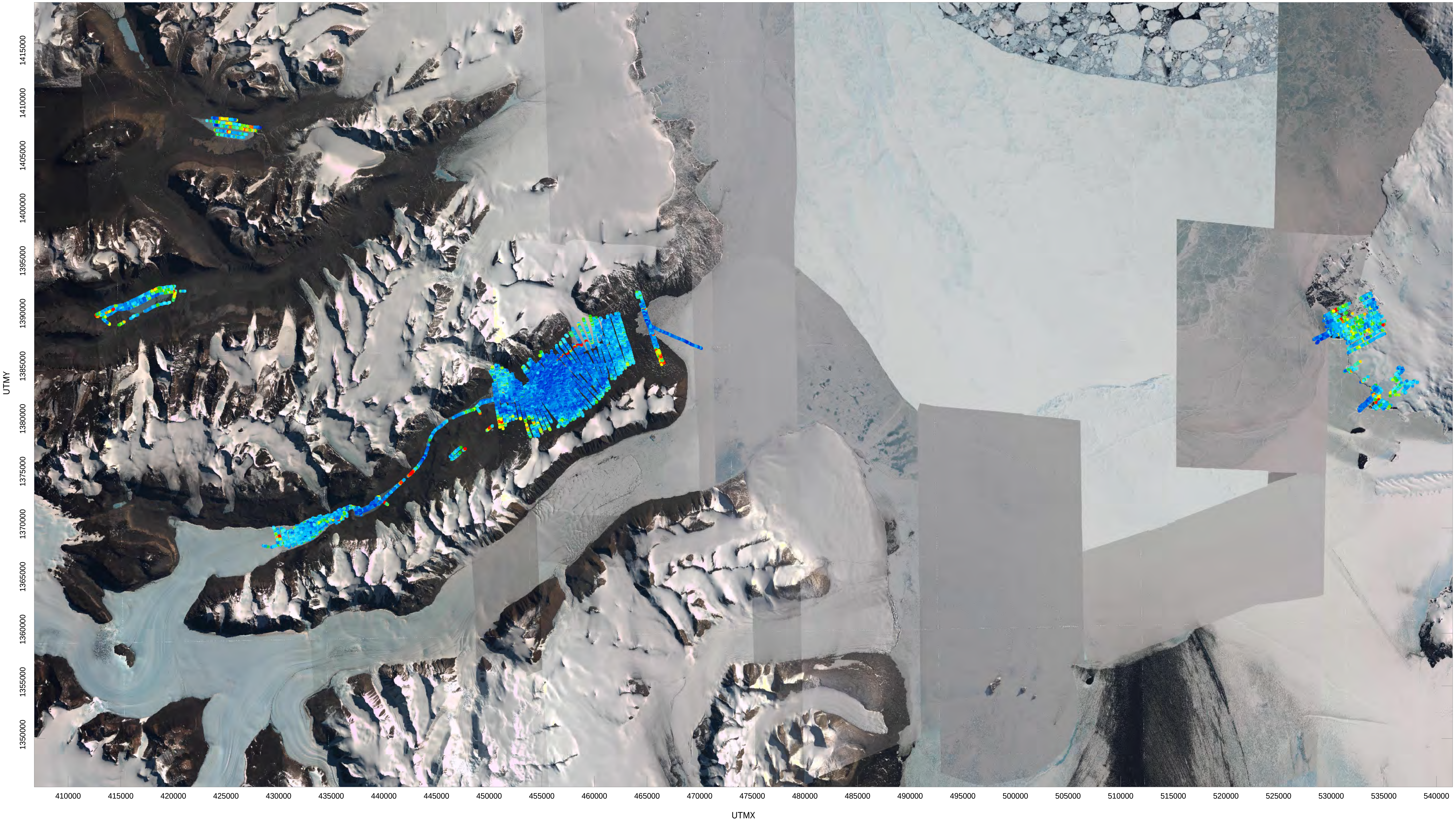

SkyTEM Survey Antartica

Data Residual

HydroGeophysics Group
AARHUS UNIVERSITY

40 km

UTM Zone 58S WGS84

0.2 0.3 0.4 0.5 0.6 0.7 0.8 0.9 1 1.1 1.2 1.3 1.4 1.5 1.6 1.7 1.8 1.9 2 2.1 2.2 2.3 2.4 2.5 2.6 2.7 2.8 2.9 3

Residual

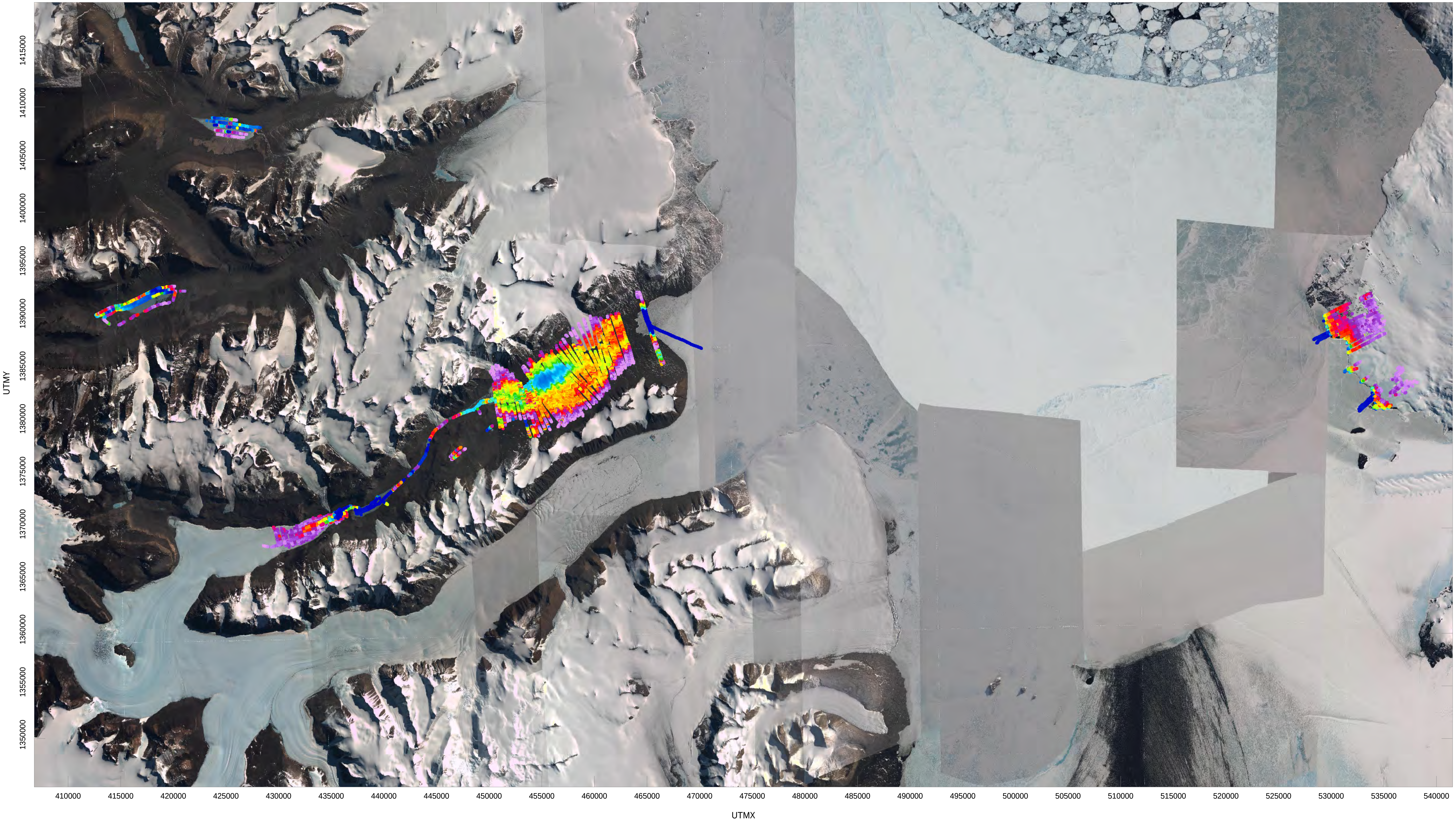

SkyTEM Survey Antartica

Depth of investigation (DOI lower)

HydroGeophysics Group
AARHUS UNIVERSITY

40 km

UTM Zone 58S WGS84

100 200 300 400 500 600
Depth [m]

APPENDIX II: DIGITAL DELIVERIES

In the next pages you will find information about the organization of the survey workspace and some explanations about how to use it. To have access to those data, please send a request to:

esben.auken@geo.au.dk

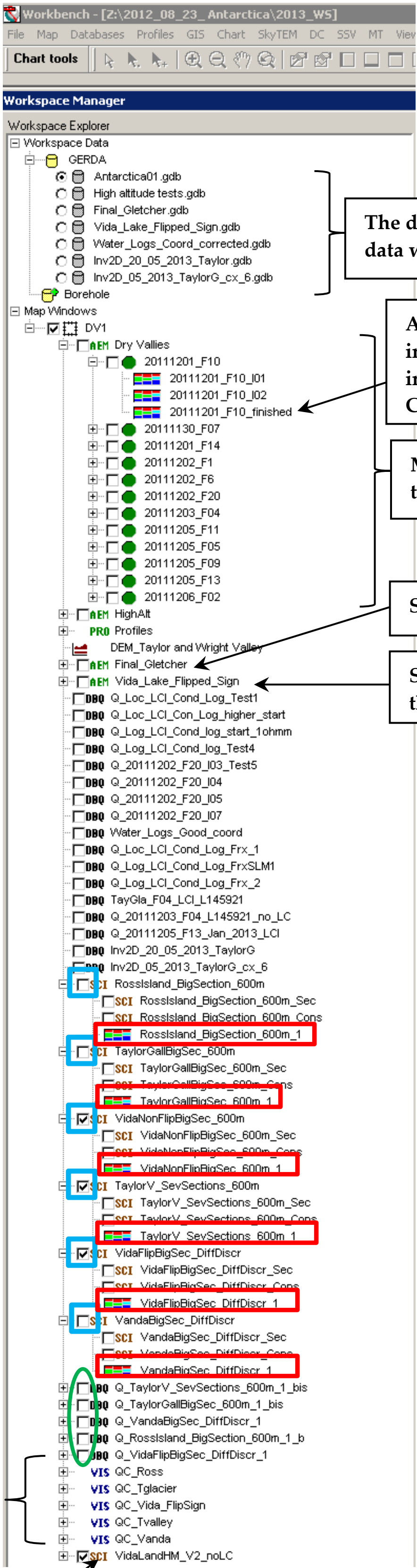

The data base files which contain the SkyTEM processed data with results from Laterally Constrained Inversion (LCI)

A LCI node result for one the flight. IMPORTANT: these inversion results are used for data processing and checking. The final results you have to use is from Spatially Constrained Inversion (SCI)

Main Sky node which contains most of the flights of the survey

Sky node for Ross Island/Gletcher

Sky node for Lake Vida (we had to reimport these data because of a problem of sign)

You can click on these boxes to see where it is located on the map

The SCI results you are going to use for interpretation.

The "smooth" inversions or the node names with "29L" in it are inversions with 29 layers whose thicknesses are fixed during the inversion (the thicknesses increase progressively with depth) and where resistivities of the thin layers are vertically constrained so that there is no big unrealistic "jump". The reason why this multi-layered inversion is also called smooth inversion.

Data Base Query (DBQ) nodes

These ones already contain gridded maps from the SCI results (kriging).

But I show you in the next page how you can export the SCI results directly as XYZ ascii files you can use later for analysis in Matlab for ex.

Quality Control (QC) nodes, e.g. like data residual, cf. QC maps in Appendix I of the survey report.

An attempt has been made to invert the data acquired on land around Vida Lake (whose sign is opposite compared to data acquired above the lake), but the ground is too resistive to give really reliable TEM signal; only less than 4-5 gates remain in the high moment (HM) curve.